The Characteristics of a Hydrogenated Amorphous Silicon Semitransparent Solar Cell When Applying n/i Buffer Layers

Da Jung Lee, Sun Jin Yun, Seong Hyun Lee, and Jung Wook Lim

In this work, buffer layers with various conditions are inserted at an n/i interface in hydrogenated amorphous silicon semitransparent solar cells. It is observed that the performance of a solar cell strongly depends on the arrangement and thickness of the buffer layer. When arranging buffer layers with various bandgaps in ascending order from the intrinsic layer to the n layer, a relatively high open circuit voltage and short circuit current are observed. In addition, the fill factors are improved, owing to an enhanced shunt resistance under every instance of the introduced n/i buffer layers. Among the various conditions during the arrangement of the buffer layers, a reverse V shape of the energy bandgap is found to be the most effective for high efficiency, which also exhibits intermediate transmittance among all samples. This is an inspiring result, enabling an independent control of the conversion efficiency and transmittance.

Keywords: Transparent solar cell, amorphous silicon solar cell, n/i buffer layer, color PV window.

I. Introduction

Green energy sources have been widely researched owing to the exhaustion of fossil fuels and the rise of environmental pollution. Among the types of green energy sources, the solar cell has taken center stage based on several advantages, including being pollution-free and an eternal energy resource. Building-integrated photovoltaics (BIPV) have attracted a great deal of attention as popular applications of solar cells because they offer an elegant way to install the required amount of PV systems without the use of additional land. For a semitransparent solar window in a BIPV, a dye-sensitized solar cell (DSSC) that can be semitransparent with various colors has been primarily investigated [1]. However, DSSCs have thus far been hindered due to degradation of the dye at elevated temperature and dissolution of the platinum counter electrode [2].

In an effort to ensure stability, hydrogenated amorphous silicon (a-Si:H) can be used as a substitute for a DSSC since it has numerous inherent advantages for BIPV applications [3]. For instance, stable a-Si:H film can be deposited uniformly by a chemical vapor deposition (CVD) method, and the energy required in manufacturing a a-Si:H solar cell is much less than that required for a crystalline silicon solar cell owing to its low process temperature (200°C to 400°C).

Until now, most semitransparent a-Si:H solar structures have been focused on aperture types [4]. Thus, in spite of the advantages mentioned above, the conversion efficiency of an aperture-type a-Si:H semitransparent cell would be severely reduced if the transmittance (T) were enhanced.

Therefore, it is difficult to control the T and efficiency (η) independently, owing to the tradeoff relationship between them. To overcome this limitation, our group fabricated a penetration-type solar cell. In a penetration-type solar cell, most areas of the cell simultaneously generate electricity and transmit light, which implies that we can enhance the T without compromising the conversion efficiency. One of the methods used to realize the enhancement of T and η is to employ buffer layers at the p/i or n/i interface. In our previous work, to enhance the T and η, a-Si:H buffer layers were inserted at the

Manuscript received Sept. 12, 2012; revised Apr. 18, 2013; accepted May 10, 2013.

This work was supported by the New and Renewable Energy Development Project (2010T100100749) and the Energy International Collaboration Project (2011-8520010-040) of the Korea Ministry of Knowledge Economy.

Da Jung Lee (phone: +82 42 860 0917, v0516v@etri.re.kr), Sun Jin Yun (sjyun@etri.re.kr), Seong Hyun Lee (dalsimlee@etri.re.kr), and Jung Wook Lim (limjw@etri.re.kr) are with the Components & Materials Research Laboratory, ETRI, Daejeon, Rep. of Korea.

http://dx.doi.org/10.4218/etrij.13.0212.0402

p/i interface [5].

Thus far, to improve the solar cell performance, such as the open circuit voltage (V_{OC}), short circuit current (J_{SC}), and fill factor (FF), regardless of the T, many groups have also carried out studies on p/i buffer layers. Such research, however, has focused only on an improvement of the conversion efficiency [6]. Inserting p/i buffer layers with a wide optical bandgap results in not only preventing an electron back recombination but also an enlarging of the internal field, which helps enhance the V_{OC} and FF without a reduction in the T in the visible region. In our previous study, we also achieved an enhancement in T as well as η by adopting multiple p/i buffer layers [5].

II. Experiment

Various combinations of buffer layers with different bandgaps are prepared to investigate the role of buffer layers. In addition, the T of a solar cell is analyzed for the application of a solar window. The p-a-Si:H, i-a-Si:H, and n-a-Si:H layers and a-Si:H buffer layers are deposited using inductively coupled plasma CVD. The process temperature is 250°C, and the working pressure is 0.2 torr. For the measurement of I-V, the incident light is from the p side, and our solar cell structure is superstrate. Also, gallium-doped zinc oxide is used for the transparent conductive oxide (TCO) and is deposited using an rf-magnetron sputter method. To secure the transparency on both sides of the cell, TCO is deposited and used as top and bottom electrodes with a thickness of 500 nm and 800 nm, respectively. For a semitransparent solar cell, the thickness of the absorbing a-Si:H layer is fixed to as low as 150 nm to obtain high T, and the electrode area is 0.25 cm × 0.25 cm.

III. Results and Discussion

To vary the optical bandgap of the buffer layers, we use various hydrogen dilution ratios (R), which are defined as $[H_2]/[SiH_4]$, that is, the ratio of flow rates of hydrogen (40 sccm to 160 sccm) and silane gases (40 sccm) in the fabrication of buffer layers. The bandgap of n/i buffer layers is varied from 1.67 eV to 1.78 eV (R=10 to R=1). The p/i buffer layers with a wide bandgap are also introduced for all samples. A general a-Si semitransparent solar cell structure and six configurations of buffer layers are considered in Fig. 1. As described in this figure, Cell 1 has no buffer layer and Cells 2, 3, and 4 have triple buffer layers in the following sequences of R values from the intrinsic side to the n side: R=1-3-6, R=6-3-1, and R=6-1-3, respectively. The thickness of one buffer layer is about 3 nm, and the total thickness is approximately 10 nm in the case of triple buffer layers. The thickness of Cell 5, which has the same

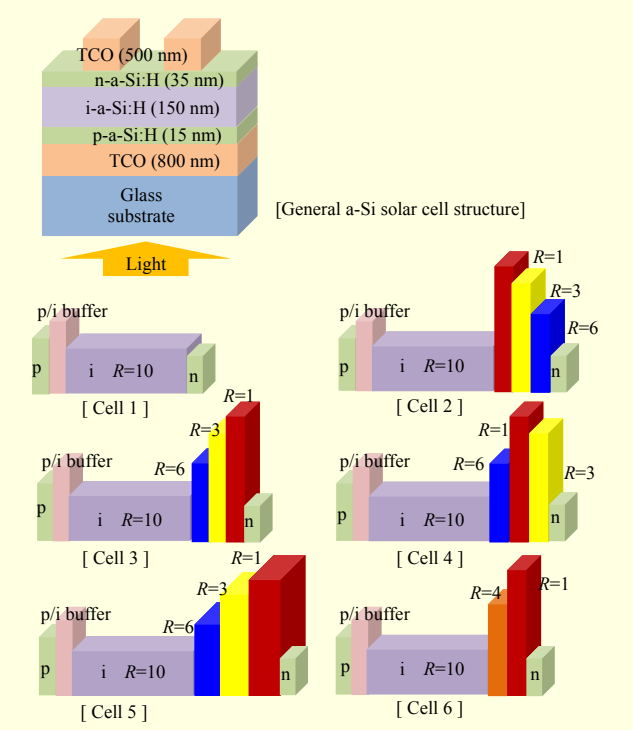

Fig. 1. Structures with various combinations of buffer layers at n/i interface in our experiments.

Table 1. Performances of fabricated solar cells with various combinations of buffer layers. Measurement condition: 25°C, 1,000 W/m^2, and initial efficiency.

	V_{OC} (V)	J_{SC} (mA/cm^2)	FF (%)	Initial efficiency (%)
Cell 1	0.826	11.36	64.2	6.03
Cell 2	0.761	11.40	68.6	5.95
Cell 3	0.818	11.55	69.3	6.55
Cell 4	0.824	11.41	70.3	6.61
Cell 5	0.792	11.35	70.4	6.32
Cell 6	0.805	11.34	68.3	6.23

sequence of R values as Cell 3, is about 15 nm, while Cell 6 has dual buffer layers of R=4-1 with a total thickness of about 10 nm. Except the buffer layers, all conditions are kept constant. In all cases, reasonable T is obtained in the visible region. The main performances of solar cells with various combinations of buffer layers are listed in Table 1.

When a-Si:H films are deposited at a low R, they exhibit a wide bandgap and contain more defects. Despite the demerits related to a dangling bond, it is quite advantageous for a-Si:H films with a wide bandgap to be applied as buffer layers with respect to the carrier collection and formation of an internal electrical field. Therefore, in practice, the FF is expected to be

enhanced mainly owing to an increase in the shunt resistance (R_{sh}).

It is generally known that a zone with negatively charged dangling bonds (D^-), adjoining the n layer, is quite substantial, and that this zone will have a decisive effect in deforming the internal electric field, which degrades the V_{OC}. Therefore, the neutralization of these D^- through hole carriers is an important factor for obtaining a high V_{OC} [7]. Therefore, the bandgap arrangement influences the collection of holes in the valence band at the n layer or neutralizes D^- to become D^0, which dominates the V_{OC}. Comparing Cell 2 with Cell 3, the buffer layer adjacent to the intrinsic layer at the n/i interface has the wider optical bandgap in Cell 2. In Cell 3, a photo-generated hole can more easily be transferred to the n side due to having a smaller barrier than that of Cell 2. Therefore better neutralization occurs in Cell 3 than in Cell 2 due to the significant recombination of D^-.

As shown in Table 1, Cell 2 shows the lowest V_{OC} among all samples. Meanwhile, Cell 3 shows a relatively high V_{OC} with a reverse bandgap arrangement, as illustrated in Fig.1. The defects within the buffer layers, which are lower in quality than the intrinsic layer, trap electrons when the buffer layers are inserted between the intrinsic layer and n layer. Therefore, in spite of an increase in the internal field, J_{SC} of Cell 2 does not show a remarkable increase in comparison to Cell 1.

On the other hand, owing to a gradual change in the bandgaps of the buffer layers and an improved internal field, free carriers jump over barriers easily, which results in an improved J_{SC} of Cell 3 compared to that of Cell 1. In the case of Cell 5, despite the same structure as Cell 3, the values of V_{OC} and J_{SC} are reduced as an increase in the thickness of the buffer layers leads to an increase in the probability of defects from low-quality layers. Therefore, in the arrangement of the buffer layers, proper thickness is required to improve the cell's performance [8].

Comparing Cell 3 of the triple buffer layers and Cell 6 of the dual buffer layers, both V_{OC} and J_{SC} are higher in Cell 3, which may be ascribed to a lower field and a less effective arrangement of the energy barrier for carrier collection in Cell 6. Among the solar cells with various buffer layers, Cell 4 with a reverse V shape of the bandgaps shows the best conversion efficiency. It has been reported that FF increases remarkably when the n/i buffer layer forms a reverse V shape [8].

Figure 2 illustrates the external quantum efficiency (EQE) spectra for all samples. Generally, the QE curves in a long wavelength reflect the properties of carrier collection near the n/i interface when light is illuminated from the p side. Comparing the QE results of Cell 2 and Cell 4 with those of Cell 1, as shown in Fig. 2, Cell 2 uses light more effectively than Cell 1 below 500 nm, while the QE curves are almost

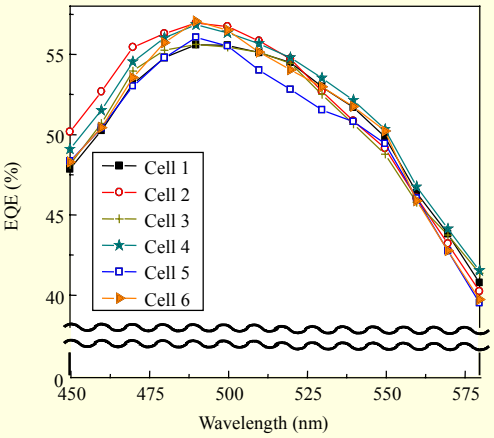

Fig. 2. QE spectra of fabricated solar cells with various buffer layers.

Table 2. R_{sh}, R_{seri}, and T of fabricated solar cells with various buffer layer conditions. R_{sh}: short-circuit differential resistance [=R_{sc}].

	R_{sh} (Ω)	R_{seri} (Ω)	Average T (%) in 400 nm to 800 nm
Cell 1	2,300	34	20.9
Cell 2	4,800	32	19.6
Cell 3	4,400	32	19.1
Cell 4	6,600	32	18.9
Cell 5	5,100	29	17.6
Cell 6	4,500	36	17.7

identical at a longer wavelength. On the contrary, Cell 4 shows a remarkable improvement of QE at above 550 nm in comparison with Cell 1, and it is believed that, through this result, carrier collection near the n/i interface is strongly dependent on the arrangement of n/i buffer layers.

Table 2 shows the R_{sh}, series resistance (R_{seri}), and average T in the visible region (400 nm to 800 nm) of all samples. The R_{seri} values are almost identical for all samples, whereas the R_{sh} between cells is significantly different. Thus, the FF is improved due to an improved R_{sh} for all insertions of n/i buffer layers. Among all the cells, the R_{sh} of Cell 4 shows the highest value. This implies that the most effective internal field might be generated in the structure of the reverse V shape of the bandgap of Cell 4.

For the fabrication of a semitransparent solar cell, it is necessary to overcome the tradeoff between T and η. Hopefully, when inserting the buffer layers at the p/i interface, the transmittance and efficiency simultaneously increase [5].

On the contrary, the T somewhat decreases along with the

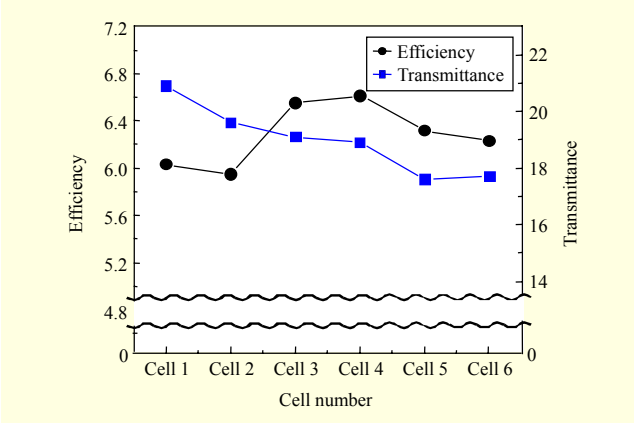

Fig. 3. Efficiency and transmittance curves for all samples with various buffer layer configurations.

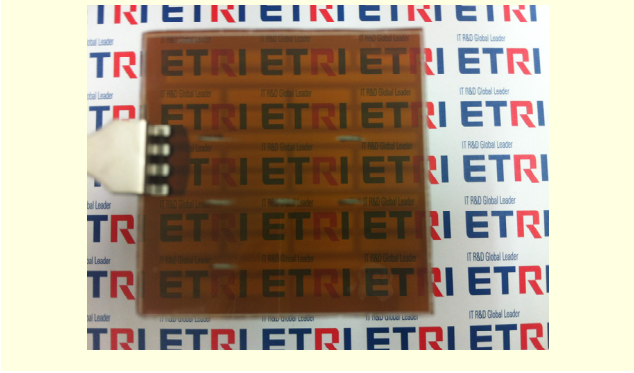

Fig. 4. Photo of penetration-type solar Cell 4 with buffer layers at n/i interface.

efficiency when the n/i buffer layers are inserted. It is plausible that visible light in a longer wavelength may be absorbed. In the case of Cell 5, in spite of its similar structure to Cell 3, the T is reduced further owing to the absorption loss by the thicker layers. There is little difference in T for various configurations of buffer layers. However, the thickness of buffer layers strongly affects the T. Cells 3 and 5 have the same configuration of buffer layers, but Cell 5 shows a lower transmittance than Cell 3 because Cell 3 has thinner buffers.

The relationship between the T and η with respect to our penetration-type semitransparent solar cell when introducing n/i buffer layers is shown in Fig. 3. Generally, the T and η have a tradeoff relationship in a semitransparent solar cell. However, Cells 3 and 4, which show high η, possess intermediate T, indicating a deviation from the tradeoff relationship. Thus, the n/i buffer layers allow for independent control of the T and η.

Figure 4 shows Cell 4, which demonstrates a relatively high average T of 18.9% in visible wavelengths. In particular, the maximum T is as high as 40.2% at a wavelength of 780 nm. Hence, the insertion of the buffer layer is believed to be helpful in obtaining a higher η without a remarkable decrease in T.

IV. Conclusion

In summary, several combinations of buffer layers were applied at the n/i interface in a-Si:H semitransparent solar cells to improve the performance of a solar cell. It was observed that the performance of a solar cell strongly depends on the arrangement and thickness of the buffer layers. From the neutralization of a charged dangling bond by a hole, a high V_{OC} is maintained without significant degradation. Owing to the formation of internal fields near the n/i interfaces, the R_{sh} increases, resulting in an increase in the FF. Moreover, J_{SC} depends on how the band of buffer layers is arranged and is increased when the buffer layers are placed in ascending order from the i layer to the n layer, which proves effective electron collection. Among all combinations of n/i buffer layers, a reverse V bandgap shape was found to be suitable to obtain a high internal field. With respect to the transparency, triple buffer layers were found to be more advantageous than dual layers. Furthermore, the cell with the highest η among all samples had an intermediate T. This result implies that it is possible to independently control the T and η.

References

[1] S. Yoon et al., "Application of Transparent Dye-Sensitized Solar Cells to Building Integrated Photovoltaic Systems," *Building Environ.*, vol. 46, no. 10, Oct. 2011, pp. 1899-1904.

[2] W.J. Lee et al., "Grid Type Dye-Sensitized Solar Cell Module with Carbon Counter Electrode," *J. Photochem. Photobio. A: Chem.*, vol. 194, no. 1, Feb. 2008, pp. 27-30.

[3] J.H. Yoon, J.H. Song, and S.J. Lee, "Practical Application of Building Integrated Photovoltaic (BIPV) System Using Transparent Amorphous Silicon Thin-Film PV Module," *J. Solar Energy*, vol. 85, no. 5, May 2011, pp. 723-733.

[4] Y.C. Lin et al., "Comparison of AZO, GZO, and AGZO Thin Films TCOs Applied for a-Si Solar Cells," *J. Electrochem. Soc.* vol. 159, no. 4, Apr. 2012, pp. 599-604.

[5] J.W. Lim, D.J. Lee, and S.J. Yun, "Semi-transparent Amorphous Silicon Solar Cells Using a Thin p-Si Layer and a Buffer Layer," *ECS Solid State Lett.*, vol. 2, no. 6, Mar. 2013, pp. Q1-Q3.

[6] B. Vet and M. Zeman, "Relation between the Open-Circuit Voltage and the Band Gap of Absorber and Buffer Layers in a-Si:H Solar Cells," *J. Thin Solid Films*, vol. 516, no. 20, Aug. 2008, pp. 6873-6876.

[7] A. Shah, Ed., *Thin-Film Silicon Solar Cells*, Lausanne, Switzerland: EPFL Press, 2010.

[8] D. Lundszien, F. Finger, and H. Wagner, "a-Si:H Buffer in a-SiGe:H Solar Cell," *J. Solar Energy Mater. Solar Cells*, vol. 74, no. 1-4, Oct. 2002, pp. 365-372.